Fluorescence and Phosphorescence from Individual C$_{60}$ Molecules Excited by Local Electron Tunneling

Elizabeta Ćavar,[1] Marie-Christine Blüm,[1] Marina Pivetta,[1] François Patthey,[1]
Majed Chergui,[2] and Wolf-Dieter Schneider[1]

[1]*Institut de Physique des Nanostructures, Ecole Polytechnique Fédérale de Lausanne (EPFL), CH-1015 Lausanne, Switzerland*
[2]*Laboratoire de Spectroscopie Ultrarapide, ISIC, Ecole Polytechnique Fédérale de Lausanne (EPFL),
CH-1015 Lausanne, Switzerland*

Using the highly localized current of electrons tunneling through a double barrier scanning tunneling microscope junction, we excite luminescence from a selected C$_{60}$ molecule in the surface layer of fullerene nanocrystals grown on an ultrathin NaCl film on Au(111). In the observed fluorescence and phosphorescence spectra, pure electronic as well as vibronically induced transitions of an individual C$_{60}$ molecule are identified, leading to unambiguous chemical recognition on the single-molecular scale.

Light emission induced by electrons tunneling through the junction formed by the sample and the tip of a scanning tunneling microscope (STM) has been proposed to characterize the optical properties of nanoscale objects at surfaces [1]. Contrary to conventional nonlocal techniques, the local character of this method offers the unique possibility to select and probe individual atoms, molecules, or clusters on surfaces.

Photon emission due to the decay of localized surface plasmons, excited by inelastic electron tunneling (IET), has been observed on metal surfaces [2,3], as well as on supported metallic nanoparticles [4]. Luminescence spectra have been acquired from semiconductor heterostructures [5] and quantum well states of metallic films [6]. Recently, luminescence from supported molecules has been obtained [7,8] by successfully decoupling them from the metallic substrate to avoid quenching of the radiative transitions [9,10], using either a thin oxide film [7] or several molecular layers [8].

However, unambiguous chemical identification of single complex molecules requires the observation and identification of *several* vibrational and/or electronic-vibrational transitions, which are the spectroscopic fingerprint of the species. Here we present the first observation of energy resolved luminescence from an individually selected C$_{60}$ molecule excited by electrons tunneling through a double barrier STM junction. A comparison with the luminescence spectra obtained by nonlocal laser spectroscopy from dispersed C$_{60}$ molecules in rare gas and glass matrices [11–16] and from solid C$_{60}$ [17–19] enables us to demonstrate the molecular origin of the detected light and to identify the observed spectral features with pure electronic transitions and with vibronic transitions induced via Jahn-Teller (JT) and Herzberg-Teller (HT) coupling [20,21]. The present novel observation of both fluorescence (singlet-to-singlet transitions) *and* phosphorescence

(triplet-to-singlet transitions) constitutes a solid basis for the chemical identification of an individual C$_{60}$ molecule.

C$_{60}$ nanocrystals were grown on NaCl layers deposited onto a Au(111) substrate. NaCl was evaporated from a Knudsen cell on a clean Au(111) surface at room temperature. Subsequently, the C$_{60}$ molecules were sublimated on the NaCl covered substrate. The experiments were performed with a homebuilt ultrahigh vacuum (UHV) STM operating at a temperature of 50 K, using cut PtIr tips. The photons emitted from the tunnel junction were collected by a lens placed inside the cryostat, guided through an optical system outside the UHV chamber to the spectrograph, and detected by a CCD camera. The wavelength resolution of the experiment was 8 nm, corresponding to ≈20 meV in the energy range of interest. The spectra were acquired with closed feedback loop while tunneling over a defined position on the sample, e.g., over a single molecule, with a typical acquisition time of 300 s. Bias voltages *V* refer to the sample voltage with respect to the tip.

NaCl forms (100)-terminated islands on Au(111) of thickness between 1 and 3 monolayers and width up to 1 μm. Contrary to the layer-by-layer growth of C$_{60}$ on Au(111) leading to extended islands found by STM [22], on NaCl electron microscopy studies [23] revealed that the C$_{60}$ molecules aggregate into hexagonal or truncated triangular nanocrystals with a height of several molecular layers. This situation is well illustrated in the STM image of Fig. 1, where C$_{60}$ islands grown on both the bare Au(111) (**A**) and the NaCl covered surface (**B–D**) are visible. The nanocrystals present a minimum height of two layers of C$_{60}$ molecules (island **B**). The nucleation of the C$_{60}$ nanocrystals starts at defects of the NaCl layer (protrusions or vacancies), monatomic steps of Au(111) (covered with NaCl), or edges of the second layer of NaCl. As shown in Fig. 1(b), the C$_{60}$ molecules form hexagonally arranged layers with an intermolecular distance of 1 nm.
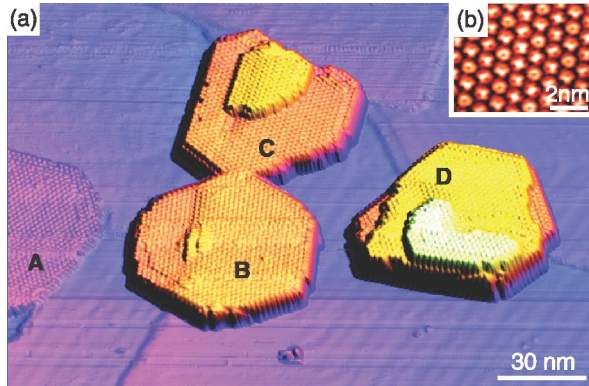
FIG. 1 (color). (a) STM image of C_{60} nanocrystals formed on a NaCl ultrathin film grown on Au(111) ($V = -3$ V, $I = 0.02$ nA). Island **A** is a C_{60} monolayer on Au(111); the small blue triangle below **A** is part of the bare Au surface. Hexagonal island **B** and truncated triangular islands **C** and **D** consist of up to two, three, and four C_{60} molecular layers, respectively, on NaCl. (b) Submolecular resolution on island **B** ($V = -3$ V, $I = 0.1$ nA).

Figure 2 shows STM-induced optical spectra from the bare Au(111) surface, the NaCl covered Au(111) surface, and from a C_{60} nanocrystal. Photons emitted from Au(111) originate from an IET process, involving excitation and decay of a surface plasmon localized between the tip and the surface [2,3,24]. A similar spectral shape is observed with reduced intensity above the dielectric NaCl spacer layer. Characteristic for this process is the energy-dependent quantum cutoff [2] (not shown) and the possibility to excite the emission with both bias polarities [3], as shown in Fig. 2. The third spectrum in Fig. 2(a) was
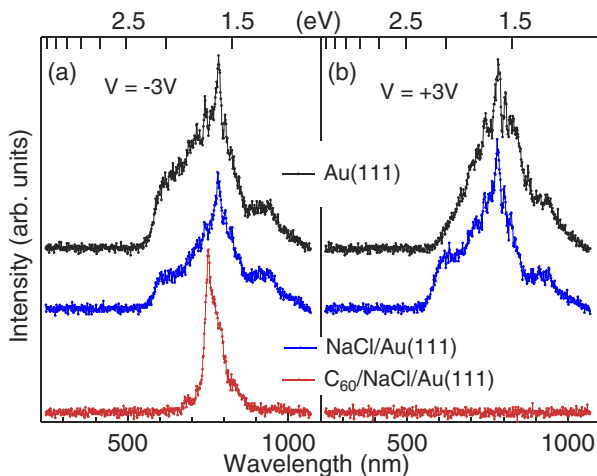

FIG. 2 (color online). STM-induced photon emission spectra acquired with (a) negative ($V = -3$ V, $I = 1$ nA) and (b) positive ($V = +3$ V, $I = 1$ nA) bias polarity. Spectra acquired on bare Au(111) and on NaCl thin film reveal characteristic emission from a localized surface plasmon. Emission from C_{60} can be excited only at negative voltages. Spectra are vertically shifted for clarity.

acquired over a single C_{60} molecule in the surface of a nanocrystal ($V = -3$ V, $I = 1$ nA). Light emission from C_{60} is observed only for bias higher than the threshold voltage of $V = -2.3$ V. The emission onset is located at ≈ 680 nm and its position is independent of the voltage. For positive voltages up to $+4.5$ V, no photon emission is detected. These observations clearly distinguish the light emission spectrum of C_{60} from those acquired over the substrate (Au and NaCl).

The occurrence of luminescence from the C_{60} molecule is related to the characteristics of the tunneling junction, as shown in Fig. 3. At negative bias voltage larger than -2.3 V, the highest-occupied molecular orbital (HOMO), which is completely filled for C_{60} in the ground state, is higher than the Fermi level (E_F) of the tip. The electrons are extracted from the HOMO and tunnel to the tip, while the lowest-unoccupied molecular orbital (LUMO), now lower than the Fermi level of the sample, is populated by the electrons tunneling from the substrate. Finally these electrons decay radiatively into the partially empty HOMO (hot electron or hole injection). The fact that luminescence is not observed for tunneling from the tip to the sample for voltages up to $+4.5$ V may be due to the asymmetry of the HOMO-LUMO gap with respect to E_F [25] and to the different properties of the two tunneling barriers (vacuum and NaCl) [26].

Figure 4(a) shows the same luminescence spectrum obtained from an individual C_{60} molecule as in Fig. 2(a) but corrected for the quantum efficiency of the detection system. In order to identify the electronic and vibronic transitions giving rise to the observed emission, we compare our results with laser-induced high-resolution photo-luminescence data [13,14] and with quantum chemical calculations [14,21]. It is now established that the lowest excited singlet state S_1 has mixed T_{1g}, T_{2g}, and G_g character [14]. The electric dipole transitions from this state to the ground state S_0 (A_g) are symmetry forbidden, but they occur through HT and JT electron-vibration coupling mechanisms of intensity borrowing [20,21]. The relaxation of the selection rules due to symmetry lowering in the C_{60} lattice gives rise to a very weak luminescence signal corresponding to the pure electronic (0-0) $S_0 \leftarrow S_1$ transition, found at ≈ 678 nm, as indicated in Fig. 4(a). The redshift of about 40 nm with respect to C_{60} in the gas phase is
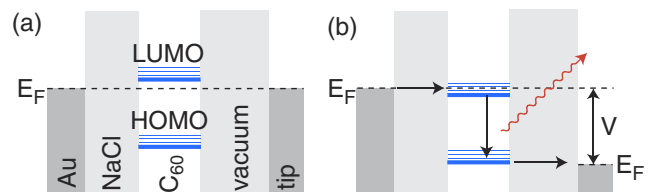

FIG. 3 (color online). Schematic energy diagram of the double barrier tunneling junction at (a) zero-bias voltage and (b) applied negative voltage, corresponding to the conditions for luminescence.
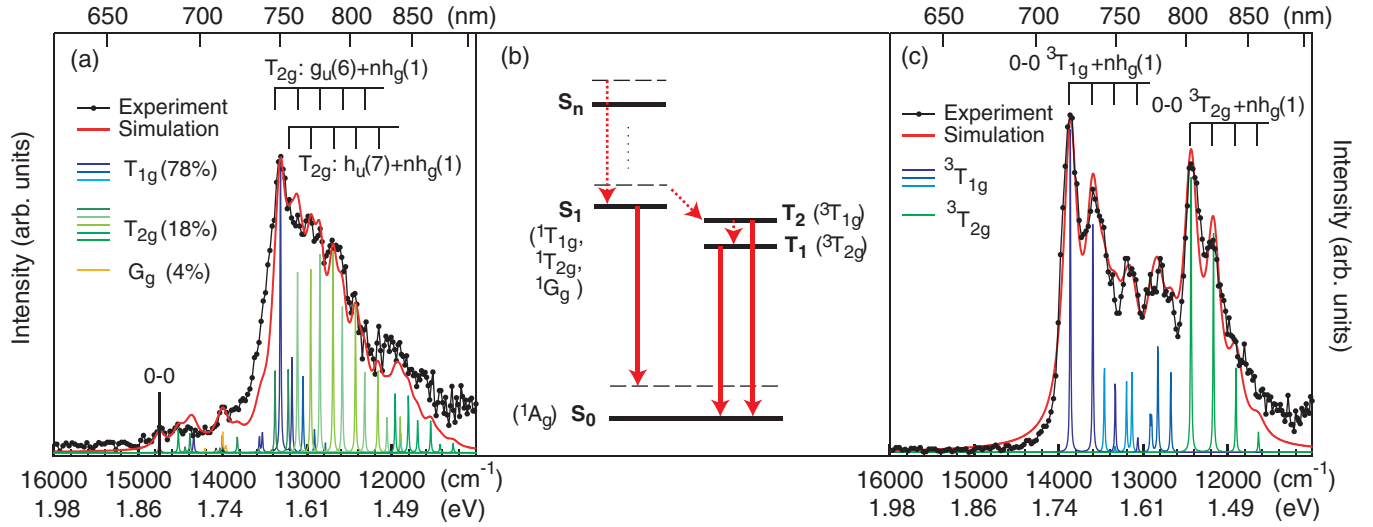
FIG. 4 (color). (a) STM-induced light emission spectrum assigned to C_{60} fluorescence ($V = -3$ V, $I = 1$ nA) and calculated spectrum. (b) Schematic diagram of the lowest singlet (S_i) and triplet (T_i) states. Horizontal solid lines: pure electronic levels; horizontal dashed lines: vibrational levels. Solid arrows represent electronic transitions; dashed arrows represent radiationless mechanisms of relaxation (internal conversion, intersystem crossing, vibrational relaxation). (c) STM-induced light emission spectrum assigned to C_{60} phosphorescence ($V = -3$ V, $I = 1$ nA) and calculated spectrum. For both simulations, experimentally determined frequencies for the vibronically induced $S_0 \leftarrow S_1$ (T_{1g}, T_{2g}, G_g) and $S_0 \leftarrow T_1$ ($^3T_{2g}$), T_2 ($^3T_{1g}$) transitions are used; see Table I [14,27]. Each component has a Lorentzian line shape, broadened by 150 cm^{-1} (a) and 200 cm^{-1} (c) to obtain the calculated spectra (red curve).

attributed to environmental effects [13,14,16]. The observation of the pure electronic origin helps to determine the vibronically induced false origins as in the high-resolution photoluminescence measurements [11,14]. The fluorescence spectra are simulated using calculated oscillator strengths and experimentally determined frequencies for the HT vibronically induced $S_0 \leftarrow S_1$ (T_{1g}, T_{2g}, G_g) transitions and the experimental frequencies for the JT active modes, as presented in Fig. 4(a) and in Table I [14,27]. The contribution of each symmetry character of S_1 varies slightly from one probed molecule to another, reflecting the known sensitivity of C_{60} to the local environment [14,18,28]. The agreement between measured and calculated spectra in Fig. 4(a) demonstrates the local character of the measurement and provides evidence for the preservation of the C_{60} molecular properties in the van der Waals

crystal, characterized by weak interactions between the molecules.

Interestingly, we also observe another type of electronic transitions, shown in Fig. 4(c). Similar spectra have been reported for laser-induced luminescence from solid C_{60} [17–19] and have recently been identified as phosphorescence originating from triplet-to-singlet ground state transitions [28]. Although symmetry and spin forbidden, intense pure electronic (0-0) triplet-to-singlet transitions have been observed in C_{60} phosphorescence spectra [12,15]. The low-energy part of the spectrum in Fig. 4(c) arises from the $S_0 \leftarrow T_1$ ($^3T_{2g}$) transition, characterized by the intense 0-0 origin at ≈ 803 nm and by the progression of a JT active mode, see Table I, in agreement with phosphorescence spectra obtained from dispersed C_{60} molecules [11,12,15]. The electronic origin is shifted by

TABLE I. HT and JT active modes used in the simulation of the STM-induced light emission spectra shown in Figs. 4(a) and 4(c). For the most intense modes contributing to the spectra, the experimental frequencies [14,27] are indicated in brackets.

Fluorescence: $S_0 \leftarrow S_1$		Phosphorescence: $S_0 \leftarrow T_1, T_2$	
S_1 (T_{1g})	HT: $t_{1u}(4)$ (1430 cm^{-1}), $h_u(7)$ (1566 cm^{-1}), $h_u(1)$, $h_u(3)$, $h_u(4)$, $t_{1u}(3)$, $h_u(5)$. JT: $h_g(7)$, $a_g(2)$, $h_g(1)$	T_1 ($^3T_{2g}$)	JT: $h_g(1)$ (266 cm^{-1})
S_1 (T_{2g})	HT: $g_u(6)$ (1410 cm^{-1}), $h_u(7)$ (1566 cm^{-1}), $g_u(1)$, $h_u(1)$, $g_u(4)$, $h_u(5)$. JT: $h_g(1)$ (266 cm^{-1}), $h_g(7)$, $a_g(2)$	T_2 ($^3T_{1g}$)	HT: $t_{2u}(3)$ (1037 cm^{-1}), $h_u(1)$, $h_u(2)$, $h_u(4)$, $a_u(1)$, $g_u(4)$, $t_{1u}(3)$. JT: $h_g(1)$ (266 cm^{-1})
S_1 (G_g)	HT: $h_u(4)$ (738 cm^{-1}), $h_u(2)$, $h_u(3)$, $g_u(3)$, $g_u(5)$, $t_{2u}(2)$		

27 nm to the red with respect to the estimated gas phase energy [12,28]. The high-energy region of the spectrum presents a similar shape, i.e., an intense transition, located at ≈ 720 nm, and a progression of vibronic bands. The observed energy difference of ≈ 0.18 eV between the two most intense features in the spectrum shown in Fig. 4(c) is in agreement with electron energy loss spectroscopy results [28,29] and with calculations [30] for the splitting of the lowest C_{60} triplet states. Therefore, the high-energy part of the spectrum in Fig. 4(c) is assigned to transitions from the next higher triplet state $S_0 \leftarrow T_2$ ($^3T_{1g}$) [28]. The good agreement between the calculated and the measured spectra allows us to assign the STM-induced phosphorescence spectrum to light emission from an individual C_{60} molecule, as in the case of fluorescence. This finding contradicts previous interpretations of similar spectra obtained by laser-induced luminescence from solid C_{60} in terms of excitonic emission [17] or emission delocalized over more than one C_{60} molecule [18,19].

The observation of both radiative relaxation processes, fluorescence and phosphorescence, in the STM-induced light emission may be related to (i) the sensitivity of the probed C_{60} molecule to the local environment in the nanocrystal and/or to (ii) the actual tunneling conditions. (i) Differences in the local C_{60} environment may induce a modification of the mixed character of the states and/or a relaxation of the selection rules, as observed in ensemble-averaged experiments [11–19,28]. Novel, here, is the fact that the influence of the environment is probed on an individual selected molecule. (ii) Even for equal nominal tunneling parameters, the actual tunneling conditions can vary from one measurement to the other. Tip shape and composition, current instabilities, or electric field fluctuation may influence the relaxation paths, for example, by enhancing the intersystem crossing and increasing the population of the triplet states. The identification of the physical origin of the observation of both fluorescence and phosphorescence calls for future time-resolved luminescence studies employing both nonlocal laser excitation and local STM-induced excitation of supported molecules.

To summarize, unambiguous chemical identification of individual C_{60} molecules is obtained via their luminescence induced by tunneling electrons. Emission from three electronic states mapping more than 20 vibrational Jahn-Teller and Herzberg-Teller modes of the molecule is identified, in excellent agreement with the known energies of the electronic [11–15,28] and vibrational [14,21,27] levels of C_{60}. The present observation of local fluorescence and phosphorescence demonstrates the capability of STM-induced light emission for the chemical recognition on the single-molecular scale.

[1] J. K. Gimzewski, B. Reihl, J. H. Coombs, and R. R. Schlittler, Z. Phys. B **72**, 497 (1988).
[2] R. Berndt, J. K. Gimzewski, and P. Johansson, Phys. Rev. Lett. **67**, 3796 (1991).
[3] R. Berndt, J. K. Gimzewski, and P. Johansson, Phys. Rev. Lett. **71**, 3493 (1993).
[4] N. Nilius, N. Ernst, and H.-J. Freund, Phys. Rev. Lett. **84**, 3994 (2000).
[5] S. F. Alvarado *et al.*, J. Vac. Sci. Technol. B **9**, 409 (1991).
[6] G. Hoffmann, J. Kliewer, and R. Berndt, Phys. Rev. Lett. **87**, 176803 (2001).
[7] X. H. Qiu, G. V. Nazin, and W. Ho, Science **299**, 542 (2003).
[8] Z.-C. Dong *et al.*, Phys. Rev. Lett. **92**, 086801 (2004).
[9] R. Berndt *et al.*, Science **262**, 1425 (1993).
[10] Z.-C. Dong *et al.*, Thin Solid Films **438–439**, 262 (2003).
[11] W.-C. Hung, C.-D. Ho, C.-P. Liu, and Y.-P. Lee, J. Phys. Chem. **100**, 3927 (1996).
[12] A. Sassara, G. Zerza, and M. Chergui, Chem. Phys. Lett. **261**, 213 (1996).
[13] A. Sassara, G. Zerza, and M. Chergui, J. Phys. B **29**, 4997 (1996).
[14] A. Sassara *et al.*, J. Chem. Phys. **107**, 8731 (1997).
[15] D. J. van den Heuvel *et al.*, Chem. Phys. Lett. **231**, 111 (1994).
[16] D. J. van den Heuvel *et al.*, J. Phys. Chem. **99**, 11 644 (1995).
[17] W. Guss *et al.*, Phys. Rev. Lett. **72**, 2644 (1994).
[18] D. J. van den Heuvel *et al.*, Chem. Phys. Lett. **233**, 284 (1995).
[19] I. Akimoto and K. Kan'no, J. Phys. Soc. Jpn. **71**, 630 (2002).
[20] F. Negri, G. Orlandi, and F. Zerbetto, J. Chem. Phys. **97**, 6496 (1992).
[21] G. Orlandi and F. Negri, Photochem. Photobiol. Sci. **1**, 289 (2002).
[22] E. I. Altman and R. J. Colton, Surf. Sci. **295**, 13 (1993).
[23] Y. Saito *et al.*, Phys. Rev. B **46**, 1846 (1992).
[24] K. Meguro *et al.*, Phys. Rev. B **65**, 165405 (2002).
[25] R. W. Lof *et al.*, Phys. Rev. Lett. **68**, 3924 (1992).
[26] S. W. Wu *et al.*, Phys. Rev. Lett. **93**, 236802 (2004).
[27] V. Schettino, P. R. Salvi, R. Bini, and G. Cardini, J. Chem. Phys. **101**, 11 079 (1994).
[28] M. Chergui (to be published).
[29] G. Gensterblum *et al.*, Phys. Rev. Lett. **67**, 2171 (1991).
[30] I. László and L. Udvardi, J. Mol. Struct. (THEOCHEM) **183**, 271 (1989).